Microchemical Journal xxx (2008) xxx–xxx

Contents lists available at ScienceDirect

Microchemical Journal

journal homepage: www.elsevier.com/locate/microc

Thirty years of snow deposition at Talos Dome (Northern Victoria Land, East Antarctica): Chemical profiles and climatic implications

M. Severi *, S. Becagli, E. Castellano, A. Morganti, R. Traversi, R. Udisti

Department of Chemistry, University of Florence, Scientific Pole, Via della Lastruccia 3, I-50019 Sesto Fiorentino (FI), Italy

ARTICLE INFO

Article history:
Received 1 August 2008
Accepted 10 August 2008
Available online xxxx

Keywords:
Ion chromatography
Talos Dome
Principal Component Analysis
Southern Oscillation Index

ABSTRACT

The aim of this study was to use ion chromatographic methods to measure trace species under clean conditions in Antarctic snow samples. Both anionic and cationic contents of the snow samples were measured using preconcentration columns for both the ion chromatographic systems due to the low concentrations typical of Antarctic snow and ice samples. Samples were collected from a snow-pit dug in Talos Dome (East Antarctica) during the 2003–2004 Italian Antarctic Campaign to perform a preliminary survey of the site chosen for deep drilling in the framework of the TALos Dome ICE core (TALDICE) international project. Stratigraphic dating was attempted for the entire snow-pit, covering about 30 years, in order to achieve climatic information from the chemical profiles of the measured species. In particular, ions coming mainly from biogenic sources were investigated as potential markers for historical reconstruction of parameters expressing atmospheric and oceanic circulation, such as Southern Oscillation Index (SOI). For the studied period, a good correlation between biogenic species and SOI and sea-ice extent in the Ross Sea sector was observed, suggesting that these ions, as recorded in Talos Dome, can be used as markers for the reconstruction of the oceanic and atmospheric conditions in the past.

1. Introduction

Permanently ice-covered regions of the world preserve a unique and datable record of the past composition of the Earth's atmosphere due to the incorporation of trace quantities of water-soluble and insoluble substances in snow and ice during both dry and wet periods [1]. For this reason, it is possible to reconstruct the history of the atmospheric environment at a specific location through chemical analysis of snow and ice samples from snow-pits and ice cores. This kind of study has been extensively carried out all over the Antarctic ice-sheet, with several time resolutions and time-scales. However, due to the complexity of climate and vastness of this ice-sheet, work is still necessary at new sites and also at previously investigated places, particularly for short-time-scale studies, in order to better understand the recent snow-chemistry composition, as well as regional differences between different sites.

In this paper, we present the results from major ions analyses carried out on a snow-pits dug at Talos Dome (Northern Victoria Land, East Antarctica) during the 2003–2004 Italian Antarctic Expedition. This site is characterised by a mean accumulation rate of 80 mm of water equivalent (w.e.)/yr [2] and was chosen as the drilling site for a deep core in the framework of the TALDICE international project.

2. Experimental

Talos Dome (TD) is a coastal dome (Fig. 1) located in Northern Victoria Land, and represents the edge of the East Antarctic plateau. Drewry [3] determined that Talos Dome is a peripheral dome lying at the end of an ice ridge coming from Dome C. ERS-1 radar altimeter data [4] locates the dome at 159°04'E 72°22'S, at 2316 m a.s.l. TD is located 290 km from the Southern Ocean and 250 km from the Ross Sea, and the aeolian surface micro-relief is mostly of the redistribution form, with South, SSW and ESE directions generally in agreement with streamline results from the katabatic wind-field model simulation by Paris and Bromwich [5].

The site chosen for the snow-pit (159° 10' 30.9'' E, 72° 49' 04.6'' S, 2330 m a.s.l.) was close to the centre of the dome, as indicated by previous works [4,6–8]. The pit was dug by hand to a depth of 565 cm, and 231 samples were collected continuously along a vertical line with a mean resolution of 2.5 cm. Samples were collected in pre-cleaned PET vials while wearing sterile overalls and gloves. All the samples were then stored in sealed polyethylene bags and kept frozen in insulated boxes for transport to Italy. All the 231 samples were melted in a clean room under a laminar flow hood shortly before chemical analysis. The anions and cations were analysed simultaneously using two Dionex-500 ion-chromatography systems.

The anionic content [F^-, methanesulphonate anion (MSA), Cl^-, NO_3^- and SO_4^{2-}] was analysed in a single run using an AG17-4 mm guard column and an AS17-4 mm analytical column with electrochemical

* Corresponding author.
E-mail address: mirko.severi@unifi.it (M. Severi).

0026-265X/$ – see front matter © 2008 Elsevier B.V. All rights reserved.
doi:10.1016/j.microc.2008.08.004

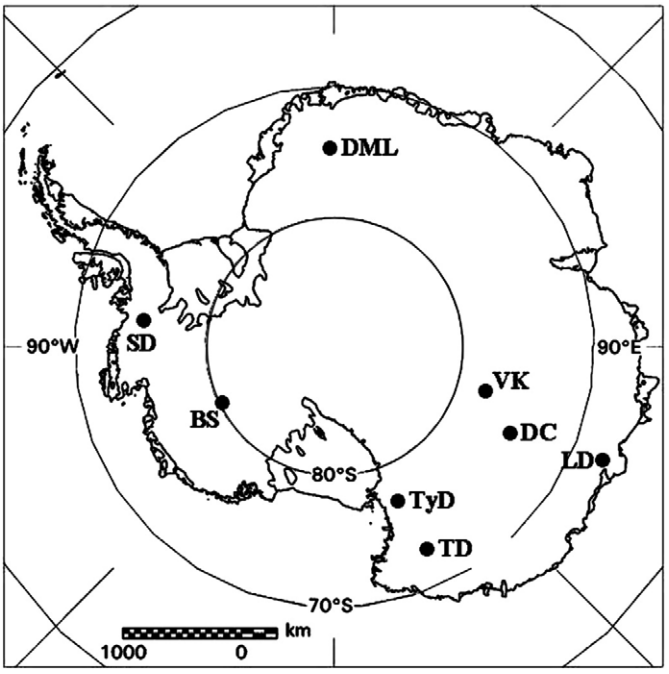

Fig. 1. Map of the sampling site together with the most important ice core drilling sites. (TD: Talos Dome, DC: Dome C, LD: Law Dome, VK: Vostok, TyD: Taylor Dome; DML: Donning Maud Land, SD: Siple Dome, BS: Byrd Station).

suppression and gradient elution. The eluent used for anion analysis was a Na_2CO_3/$NaHCO_3$ buffer solution. An example of the separation obtained under these conditions is shown in Fig. 2. The analytical performances of the method are summarised in Table 1 and further details on analytical method and performances are reported in Morganti et al. [9].

Cations (Na^+, NH_4^+, K^+, Mg^{2+} and Ca^{2+}) were determined using a CG12A-4mm guard column and a CS12A-4mm analytical column with electrochemical suppression. The eluent used for cation determination was H_2SO_4 20 mM, and a chromatogram of the cations separation is also shown in Fig. 2. Both systems were calibrated daily with 5–6 standard solutions in the concentration range of the analysed samples. The sample handling procedure was minimized using a Gilson 222 XL autosampler. All samples were filtered using an on-line 0.45 μm filter before injection into the ion chromatographic systems and pre-concentrated on Dionex TCC and TAC-2 (respectively for cations and anions) pre-concentration columns with a 50 μl dead-volume. In this way, higher sensitivities are achieved in order to easily detect the low concentrations of the analytes found in Antarctic snow samples.

In order to identify and evaluate extra sea-spray sources for Na^+ and extra crustal sources for Ca^{2+}, the sea-salt fraction of Na^+ ($ssNa^+$) and non-sea-salt Ca^{2+} were computed. $SsNa^+$ was evaluated by subtracting the crustal contribution, calculated on the basis of Ca^{2+} content, from the measured total Na^+ concentration. Since Ca^{2+} also has marine and crustal sources, its non-sea-salt fraction ($nssCa^{2+}$) had to be evaluated as well. A simple 2-equation system was used to evaluate sea-spray and crustal contribution of Na^+ and Ca^{2+}:

1) $ssNa^+ = totNa^+ - nssCa^{2+}/R_{crust}$
2) $nssCa^{2+} = Ca^{2+} - R_{sea\ water} * ssNa^+$

$(Ca^{2+}/Na^+ = 0.038 = R_{sea\ water})$ $(Ca^{2+}/Na^+ = 1.78 = R_{crust})$

where R_{crust} and $R_{sea\ water}$ are the mean ratio (w/w) in the Earth's crust and in bulk seawater, respectively [10].

Nss–SO_4^{2-} content was also computed by subtracting from total sulphate the contribution of primary sulphate (sea-salt sulphate) using $ssNa^+$ concentration as a univocal marker of the sea-spray source:

$$nssSO_4^{2-} = SO_{4\ tot}^{2-} - ssSO_4^{2-} \quad ssSO_4^{2-} = 0.253 ssNa^+$$

where 0.253 is the sea water sulphate/sodium ratio (w/w) [11].

As is usually accomplished for Antarctic precipitations [12], free acidity content was not determined by direct measurement, but calculated by the unbalance between anionic and cationic content, expressed as μeq/L.

3. Results and discussion

3.1. Mean composition of precipitation at Talos Dome and Principal Component Analysis

Table 2 reports the basic statistical parameters of the most relevant determined and calculated ($ssNa^+$, $nssCa^{2+}$, $nssSO_4^{2-}$, H^+) chemical species. Among the cationic components, Na^+ is largely dominant by weight and is confirmed as a reliable sea-spray marker, being almost exclusively constituted by the sea-salt fraction (95.7% of the total Na^+). It also shows the highest relative variability (74.1%) together with Mg^{2+} (70.6%), Cl^- (65.7%) and Ca^{2+} (67.1%) due to the occurrence of several high concentration spikes occurring most likely during winter, which can be ascribed to sea-salt storms as reported by Legrand and Delmas [13].

On the contrary, the anionic components have a more homogeneous distribution with similar contributions of Cl^-, NO_3^- and SO_4^{2-} and a minor contribution (around 3.5%) of methanesulphonate (MSA). From the ionic balance calculation, snow deposition at TD is markedly acidic, with H^+ constituting half of the cationic budget as μeq/L (50.3%).

In order to identify common sources and transport processes of chemical compounds measured in the Talos Dome snow-pit samples, a statistical treatment by Principal Components Analysis (PCA) was carried out on the dataset. PCA correlation coefficients are reported in Table 3. The first factor, which explains 43.6% of the variance, is represented by typical sea-spray components (Na^+, Cl^-, Mg^{2+}) and Ca^{2+}. The presence of Ca^{2+} together with primary marine components can be explained both by common sources and common transport processes. In fact, $ssCa^{2+}$ fraction represents a significant contribution to total Ca^{2+} budget (mean value 27.1%), indicating a relevant contribution of primary marine source. Moreover, the linear correlation between Ca^{2+} and Na^+ shows a high significance level ($P<0.01$, $R=0.653$, $n=225$) with a slope of 0.0755 ± 0.0059, roughly doubling the theoretical sea water Ca^{2+}/Na^+ ratio (0.038) and pointing out common transport processes even if an additional Ca^{2+} source with respect to sea spray is enlightened.

The second factor, related to the marine biogenic activity, includes MSA and sulphate and explains 16.4% of the system variance. The presence of sulphate in the same factor of MSA demonstrates the dominance of biogenic sources to total sulphate. Nitrate represents the third factor that explains 15.3% of the variance of the system. These first three factors together explain more than 75% of the total variance.

3.2. Seasonal pattern and stratigraphic dating

Among all the species measured in the snow-pit, MSA, nss-SO_4^{2-} and NO_3^- show a seasonal pattern, due to the seasonality of their sources.

MSA and nss-SO_4^{2-} arise from the atmospheric oxidation of dimethylsulphide (DMS), produced by phytoplankton metabolic activity [14] which blooms in summer season. While MSA originates only from marine biogenic activity, $nssSO_4^{2-}$ in Antarctica has other sources, such as volcanic and crustal emissions. Indeed, excluding the volcanic events, which are characterised by a sharp increase in

Please cite this article as: M. Severi, et al., Thirty years of snow deposition at Talos Dome (Northern Victoria Land, East Antarctica): Chemical profiles and climatic implications, Microchem. J. (2008), doi:10.1016/j.microc.2008.08.004

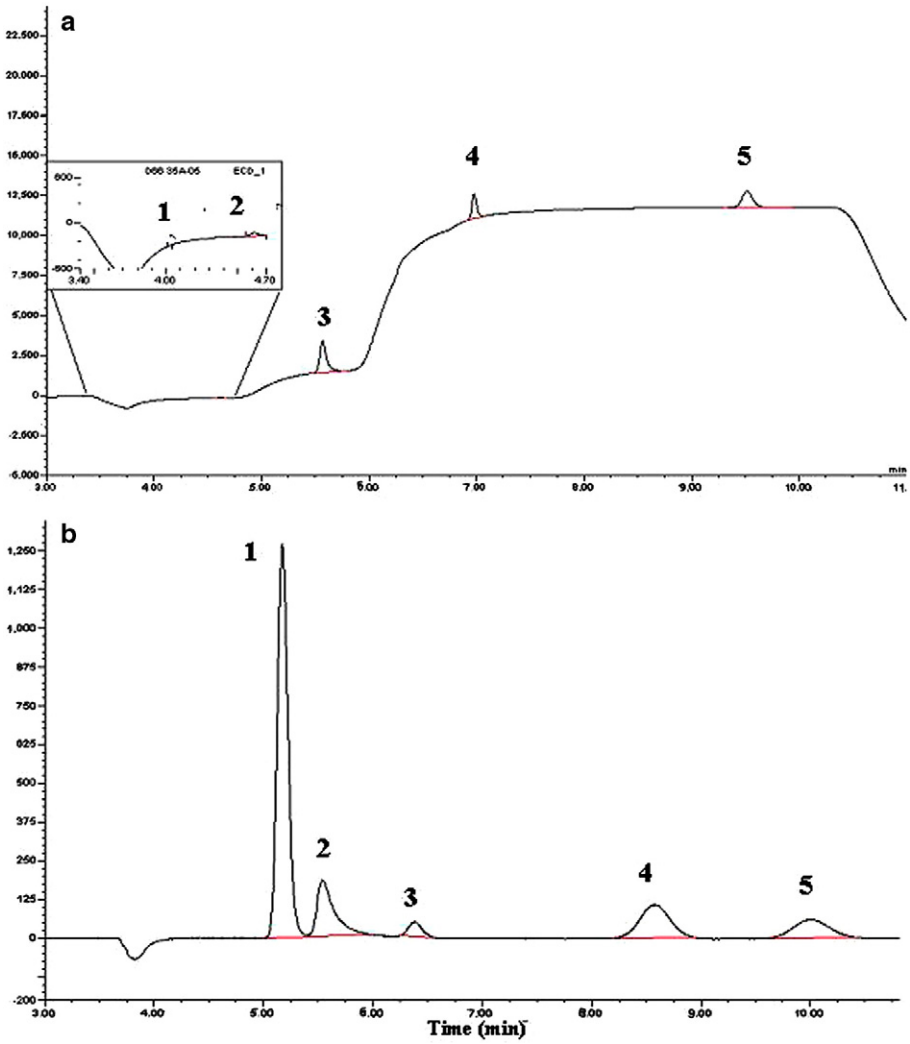

Fig. 2. Chromatographic separation of anions (a) and cations (b) obtained with the methods described in the text. Peaks relative to the measured species are marked by numbers: (a) 1. Fluoride, 2. MSA, 3. Chloride, 4. Nitrate, 5. Sulfate; (b) 1. Sodium, 2. Ammonium, 3. Potassium, 4. Magnesium, 5. Calcium.

sulphate [15,16] in a relatively short period, the dominant source for $nssSO_4^{2-}$ at Talos Dome is biogenic.

Several year-round aerosol measurements in coastal Antarctic sites [17] have shown nitrate concentration maxima during summer. The major depositional fluxes of nitrate in the Antarctic ice-sheet are supposed to be controlled by stratospheric nitrate which enters the troposphere in summer, when stratospheric/tropospheric exchanges occur [17].

The three selected markers, especially $nssSO_4^{2-}$, show a seasonal pattern with maximum concentrations occurring during summer and minima during winter.

Comparing the three concentration profiles (Fig. 3a, b, c), some peak shifts and some missing signals can be observed, and thus none of these markers represents a fully reliable signal for dating purposes. The slight phase-shift between some maxima in the biogenic (MSA and $nssSO_4^{2-}$) and in the atmospheric (NO_3^-) markers can be ascribed to a temporal shift in the maximum intensity of the source. Alternatively, this dephasing can be explained by post-depositional phenomena affecting MSA and nitrate in the snow layers, such as migration under a summer–winter concentration gradient [18,19] or re-emission of gaseous species in the up-core direction, especially in the case of high acidic content in low accumulation-rate sites [20]. Nevertheless, such post-depositional processes do not delete the seasonal trend of the three markers in this snow-pit, and they have been used to build a time-scale for the record.

The dating was accomplished by a multi-parametric approach, involving the calculation of the three normalised profiles by dividing each concentration by the maximum concentration found in a moving depth interval as large as the expected annual layer thickness. The three profiles were then summed to give a normalised sum profile

Table 1
Summary of the analytical performances of the chromatographic method for anions and cations

Ion	Na^+	NH_4^+	K^+	Mg^{2+}	Ca^{2+}	F^-	$CH_3SO_3^-$	Cl^-	NO_3^-	SO_4^{2-}
Upper limit of the linear range (μg L^{-1})	800	14	1300	700	700	16	14	600	3000	2500
Sensitivity (nS μg^{-1} L)	77	82	36	56	33	78	19	78	58	43
Reproducibility (RSD)	2.0	1.0	1.9	1.5	1.5	0.6	1.9	1.5	0.9	1.8
Detection Limit (μg L^{-1})	0.09	0.15	0.13	0.11	0.11	0.01	0.10	0.15	0.02	0.08

Please cite this article as: M. Severi, et al., Thirty years of snow deposition at Talos Dome (Northern Victoria Land, East Antarctica): Chemical profiles and climatic implications, Microchem. J. (2008), doi:10.1016/j.microc.2008.08.004

Table 2
Basic statistical parameters of the main ions determined and calculated in Talos Dome snow-pit samples

	Na^+ ($\mu g\ l^{-1}$)	$ssNa^+$ ($\mu g\ l^{-1}$)	Mg^{2+} ($\mu g\ l^{-1}$)	Ca^{2+} ($\mu g\ l^{-1}$)	$nssCa^{2+}$ ($\mu g\ l^{-1}$)	MSA ($\mu g\ l^{-1}$)	Cl^- ($\mu g\ l^{-1}$)	NO_3^- ($\mu g\ l^{-1}$)	SO_4^{2-} ($\mu g\ l^{-1}$)	$nssSO_4^{2-}$ ($\mu g\ l^{-1}$)	H^+ ($\mu g\ l^{-1}$)
No. of data	231	231	231	231	231	231	231	231	231	231	231
Min.	2.52	1.89	0.36	0.76	0.22	0.42	6.54	21.59	12.42	6.59	0.26
Max.	94.87	89.57	10.56	20.71	17.49	40.49	184.1	100.2	139.6	132.7	5.21
Mean	21.79	20.86	2.31	2.80	2.04	5.36	46.73	47.38	47.52	42.00	1.76
Median	17.24	16.05	1.84	2.35	1.72	3.15	35.72	45.90	42.90	37.42	1.62
Std. Dev.	16.14	15.72	1.63	1.88	1.59	6.61	30.72	13.49	27.47	26.80	0.83

(Fig. 3d). This procedure allows the comparison between profiles showing different absolute values and the compensation of the time shift in the summer maxima of different seasonal markers. A detailed description of the multi-parametric dating procedure is reported in Udisti [21]. The use of multiple parameters showing a seasonal pattern improves the quality of the time-scale produced by making the individuation of annual layers more robust [21–23].

Annual layers have been counted starting from the sampling year (2004) backward until 1975. Fig. 4 reports the dating results, pointing out the Pinatubo signature (1992) in the $nssSO_4^{2-}$ profile. After the conversion of snow depths into water equivalent depths on the basis of density measurements, we calculated an annual mean accumulation rate for the last 30 years at TD of 77.4 mm w.e./yr, slightly lower than the values found from two firn cores drilled in the same area in the 2001/2002 (86.6 mm w.e./yr for the 1965–2001 time period; [2]) and 1996/1997 (80.5 mm w.e./yr for the 1217–1996 time period; [24]) Antarctic Campaigns. The density measurements were carried out by inserting a steel cylinder, whose volume was exactly known, into the wall of the snow-pit. The snow recovered in this way was then stored in plastic bags and weighed in a cold lab using a Mettler PE 600 balance. The density measurements were performed every 10 cm, so that a density profile was achieved for the whole depth of the snow-pit.

3.3. Sulphur compounds–Southern Ocean Index relationship

The main sulphur cycle components found in Antarctic snow samples are sulphate and methane sulphonate (MS^-). In remote marine areas, these components arise mainly from atmospheric oxidation of dimethylsulphide (DMS), produced by phytoplankton metabolic activity. MSA does not represent any other source, except for a subordinate one represented by biomass burning [25]. On the contrary, several sources of sulfate are known in Antarctica; besides biogenic, the direct contribution of sea-spray deposition is not negligible, and volcanic and crustal aerosol contributions must also be considered. While the dominant contribution to sulphur in Greenland ice cores in recent times is anthropogenic [26–28], in Antarctica no significant anthropogenic impact on sulfate total budget could be revealed, and their dominant source is the biogenic activity.

Therefore, MSA and nss-SO_4^{2-} records in TD snow have been investigated as potential markers for historical reconstruction of parameters expressing atmospheric and oceanic circulation such as Southern Oscillation Index (SOI).

SOI is the normalised difference in surface pressure between Darwin and Tahiti, with positive extremes representing La Niña and negative extremes indicating El Niño time periods [29]. In general, smoothed time series of the SOI correspond very well with changes in ocean temperatures across the eastern tropical Pacific. The negative phase of the SOI represents below-normal air pressure at Tahiti and above-normal air pressure at Darwin. Prolonged periods of negative SOI values coincide with abnormally warm ocean waters across the eastern tropical Pacific, typical of El Niño episodes. Prolonged periods

Table 3
PCA (Principal Component Analysis) factor loadings for the measured chemical species

	Factor 1	Factor 2	Factor 3
Na^+	0.976	−0.030	−0.036
K^+	0.425	−0.399	0.478
Mg^{2+}	0.911	0.148	−0.199
Ca^{2+}	0.703	−0.049	0.313
MSA	−0.043	0.729	−0.021
Cl^-	0.947	0.078	−0.004
NO_3^-	−0.166	0.212	0.855
SO_4^{2-}	0.321	0.737	0.358
Variance	3.49	1.31	1.23
No. of data	231	231	231
Total Variance Explain (%)	43.60	16.37	15.34

Factors loadings are computed by using Varimax rotation procedure.

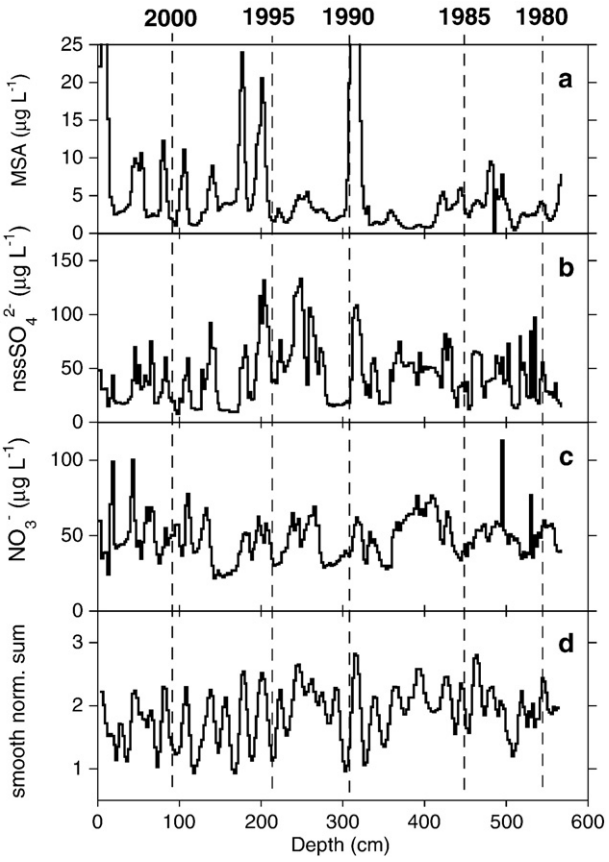

Fig. 3. MSA (plot a), $nssSO_4^{2-}$ (plot b) and NO_3^- (plot c) concentration/depth profiles. The profile in plot d was calculated by a three point running mean of summed profiles in turn obtained by summing the MSA, $nssSO_4^{2-}$ and NO_3^- (plot c) normalised profiles. Each normalised profile was calculated by dividing each analytical value k for the max value found in a chosen near interval (the interval used was $k \pm 5$). A detailed description of this multi-parametric approach for snow layers dating is reported in Udisti, 1996.

Please cite this article as: M. Severi, et al., Thirty years of snow deposition at Talos Dome (Northern Victoria Land, East Antarctica): Chemical profiles and climatic implications, Microchem. J. (2008), doi:10.1016/j.microc.2008.08.004

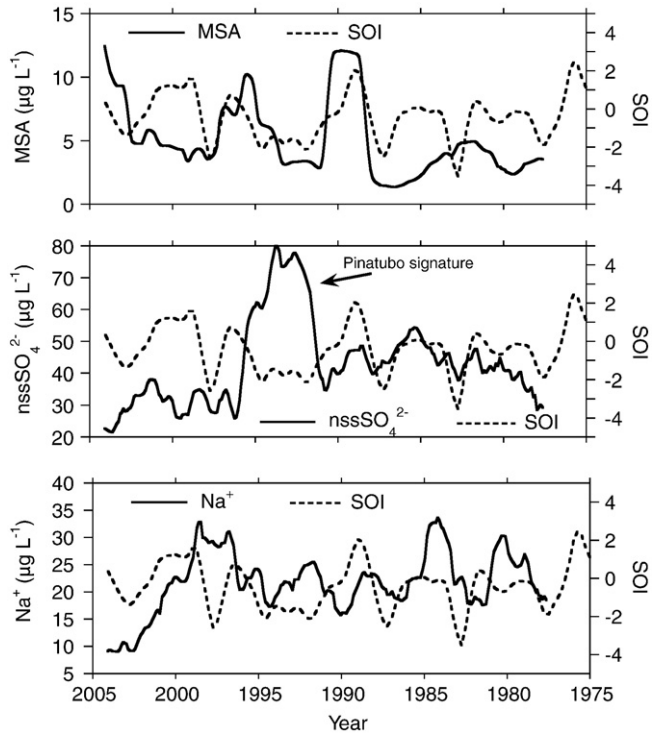

Fig. 4. Two year running mean profiles of MSA (plot a), $nssSO_4^{2-}$ (plot b) and Na^+ (plot c). In each plot also shows the SOI profile. Signature of Pinatubo eruption in $nssSO_4^{2-}$ profile is shown.

of positive SOI values coincide with abnormally cold ocean waters across the eastern tropical Pacific, typical of La Niña episodes.

In order to compare meteorological and climatic parameters to chemical stratigraphies from snow layers, there is a need to take into account that in sites with accumulation rates lower than 200 kg m^{-2} yr^{-1}, a point-to-point match is not reliable due to wind-driven redistribution processes [30]. Thus, Fig. 4a and b report MSA and $nssSO_4^{2-}$ two-year running mean profiles and SOI records (obtained from NOAA's Climate Prediction Center) for the time period covered by the snow-pit.

A good agreement between both chemical stratigraphies and SOI can be observed except for the 1991–1995 period, where a broad and high peak is evident in $nssSO_4^{2-}$ profile. Such a peak is due to the 1991 Pinatubo and Cerro Hudson volcanic eruptions and were recorded in Antarctic snow layers in 1992 [2]. For this time range, the comparison with SOI profile is not significant because sulphate volcanic sources mask the usually dominant biogenic source. Generally, nss-sulfate and MSA concentrations are higher during periods of SOI > 0 (La Niña events), while low concentration levels occur during periods of SOI < −1 (El Niño events) even if the concentration variation is not proportional to the El Niño or La Niña strength. Consequently, a significant linear correlation cannot be achieved.

The SOI influence on Antarctic atmospheric circulation has been especially studied in terms of strength and position of the Amundsen Sea Low (L_{AS}) [31–37]. According to Cullather et al. [31], in normal conditions the L_{AS} is centred close to the Eastern Ross ice-shelf and the moisture masses coming from the Ross Sea, enriched in MSA and nss-SO_4^{2-}, are directed to the TD area. During La Niña events, the low-pressure system is even stronger [36] and increases the described effect for the Ross Sea region. On the contrary, during El Niño episodes the centre of the L_{AS} is located up to 1400 km closer to the Amundsen–Bellingshausen Sea, and thus the Ross Sea does not exert a strong influence over the TD region.

Therefore, differences in transport pathways between positive and negative SOI phases may explain the observed agreement with sulphur compounds. If this is the case, a similar pattern should also be found for other marine markers. Fig. 4c shows the two-years running mean profile of $ssNa^+$ in comparison with SOI; no agreement can be observed along the entire time period. Such results can be justified by primary origin sodium, unlike secondary origin of oxidised sulphur compounds, which could lead to lower residence times in the atmosphere with respect to $nssSO_4^{2-}$ and MSA. For these reasons, the hypothesis based on transport pathways does not appear to be completely exhaustive. Alternatively, differences in source intensity can be invoked to explain the SOI-sulphur compounds relationship. Connections between Antarctic sea-ice extent and SOI have been reported [38–40]. In particular, Kwok and Comiso [41] suggested that sea ice changes in the Bellingshausen, Amundsen and Ross Sea sectors show the highest sensitivity to SOI. In its turn, sea-ice extent was found to be positively correlated to MSA concentrations from ice cores (Newall Glacier, Ross Sea region – [42]; Law Dome, Indian Ocean Sector – [43]).

The amount of sea ice melted in spring is supposed to enhance biological activity, and consequently DMS production, as suggested by Minikin et al. [44]. During the sea-ice build up in autumn, impurities and nutrients are excluded from the ice lattice and incorporated in the pack interstitial spaces (brine pockets). Gibson et al. [45] suggested that, in winter, algae cells survive in sea ice brine pockets, where the salinity is enhanced by the freezing processes. Algae cells protect themselves against the salinity and the low temperatures by producing intracellular dimethylsulphoniopropionate (DMSP), which is an osmolyte [46] and a cryoprotectant in polar waters [47]. DMSP, a precursor of DMS [14], is excreted from the cells when they experience a much lower salinity due to the sea-ice melting in spring. In addition, the stratification caused by a superficial low salinity layer covering the higher salinity seawater prevents or limits the vertical mixing, allowing the nutrients to concentrate in the superficial layers. These conditions, together with the algae release in the open seawater from the brine pockets and the increasing solar radiation, constitute positive factors for the phytoplanktonic activity, as revealed by the contemporaneous maxima of DMS concentration measured in the surface seawater [48].

Indeed, a good agreement between sea-ice extent in Ross Sea Sector and MSA and $nssSO_4^{2-}$ concentration in the TD snow-pit is shown in Fig. 5, which shows MSA and $nssSO_4^{2-}$ smoothed profiles in comparison with smoothed sea-ice extent anomalies record (obtained from NOAA's Climate Prediction Center) for the 1975–1995 time period. In spite of the short time overlapped by the three records, high

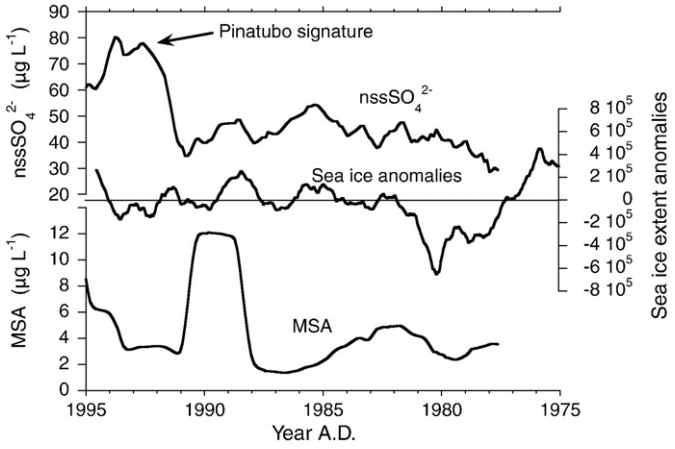

Fig. 5. Two year running mean profiles of MSA, $nssSO_4^{2-}$ and sea ice extent anomalies in the Ross Sea sector in the time period 1975–1995 A.D. Signature of Pinatubo eruption in $nssSO_4^{2-}$ profile is also shown.

Please cite this article as: M. Severi, et al., Thirty years of snow deposition at Talos Dome (Northern Victoria Land, East Antarctica): Chemical profiles and climatic implications, Microchem. J. (2008), doi:10.1016/j.microc.2008.08.004

concentration levels of sulphur compounds around 1989 and minima around 1979 correspond to positive and negative anomalies in sea-ice extent, respectively.

4. Conclusions

The preliminary site survey at Talos Dome carried on by high resolution chemical characterisation of snow-pit samples indicates that deep drilling at Talos Dome is potentially able to reconstruct hemispheric climatic changes linked to oceanic and atmospheric variations. The accumulation rate for TD, calculated via a stratigraphic dating of the pit, shows that this site will be able to yield high resolution climatic and environmental information for a relatively long time period. Moreover, our results show that MSA and nss-SO_4^{2-} records from Talos Dome ice are a reliable proxy both of the SOI changes and of the regional sea-ice variations in the Ross Sea region.

Clearly, more research is needed to fully understand the temporal and spatial variability of the SOI-Antarctic relationship; however our results confirm a strong influence (especially for the 1980s) of the ENSO on the chemical composition of the aerosol budget reaching the Talos Dome area. In addition, the results achieved in this study are in agreement with those reported by Bertler et al. [36], confirming a change in the regional atmospheric circulation pattern of the Ross Sea sector according to the L_{AS} theory.

Acknowledgements

This research was financially supported by the MIUR-PNRA program through a co-operation agreement among the PNRA consortium, University of Milano-Bicocca, and University of Venice in the framework of the “Glaciology” and “Chemistry of Polar Environments” projects. This work is an Italian contribution to the ITASE project.

References

[1] H.B. Clausen and C.C. Langway, The ionic deposits in polar ice cores. 1989. In: The Environmental Record in Glaciers and Ice Sheets, H. Oeschger and C.C. Langway Jr. (eds), John Wiley and Sons Ltd, New York, pp. 225–247.
[2] B. Stenni, M. Proposito, R. Gragnani, O. Flora, J. Jouzel, S. Falourd, M. Frezzotti, J. Geophys. Res. 107 (D9) (2002) 4076.
[3] D.J. Drewry (Ed.), Antarctica: Glaciological and Geophysical Folio, Scott Polar Research Institute, Cambridge, 1983.
[4] F. Remy, P. Shaeffer, B. Legresy, Geophys. J. Int. 139 (1999) 645.
[5] T.R. Paris, D.H. Bromwich, J. Climate 4 (2) (1991) 135.
[6] M. Frezzotti, O. Flora, S. Urbini, Terra Antartica Rep. 2 (1998) 105.
[7] M. Frezzotti, G. Bitelli, S. Gandolfi, P. De Michelis, F. Mancini, S. Urbini, L. Vittuari, A. Zirizzotti, Terra Antartica Rep. 8 (2003) 117.
[8] C. Bianchi, L. Cafarella, P. De Michelis, A. Forieri, M. Frezzotti, I.E. Tabacco, A. Zirizzotti, Ann. Geophys. 46 (6) (2003) 1265.
[9] A. Morganti, S. Becagli, E. Castellano, M. Severi, R. Traversi, R. Udisti, Anal. Chim. Acta 603 (2007) 190.
[10] H.J.M. Bowen, Environmental chemistry of the elements, Elsevier, New York, 1979.
[11] F. Maupetit, R.J. Delmas, J. Atmos. Chem. 14 (1990) 31.
[12] M. Legrand, P.A. Mayewski, Rev. Geophys. 35 (1997) 219.
[13] M. Legrand, R.J. Delmas, Ann. Glaciol. 10 (1988) 116.
[14] E.S. Saltzman, Ice Core Studies of Global Biogeochemical Cycles, NATO ASI Ser., Ser. I, vol. 30, Springer-Verlag, New York, 1995, p. 65.
[15] E. Castellano, S. Becagli, M. Hansson, M. Hutterli, J.R. Petit, M.R. Rampino, M. Severi, J.P. Steffensen, R. Traversi, R. Udisti, J. Geophys. Res. 110 (2005) D06114.
[16] E. Cosme, F. Hourdin, C. Genthon, P. Martinerie, J. Geophys. Res. 110 (2005) D03302.
[17] D. Wagenbach, F. Ducroz, R. Mulvaney, L. Keck, A. Minikin, M. Legrand, J.S. Hall, E.W. Wolff, J. Geophys. Res. 103 (D9) (1998) 10961.
[18] E.C. Pasteur, R. Mulvaney, J. Geophys. Res. 105 (D9) (2000) 11525.
[19] M.A.J. Curran, A.S. Palmer, T.D. Van Ommen, V.I. Morgan, K.L. Phillips, A.J. McMorrow, P.A. Mayewski, Ann. Glaciol. 35 (2002) 333.
[20] P. Wagnon, R.J. Delmas, Legrand, J. Geophys. Res. 104 (D3) (1999) 3423.
[21] R. Udisti, Int. J. Environ. Anal. Chem. 63 (1996) 225.
[22] S.O. Rasmussen, K.K. Andersen, A.M. Svensson, J.P. Steffensen, B.M. Vinther, H.B. Clausen, M.L. Siggaard-Andersen, S.J. Johnsen, L.B. Larsen, D. Dahl-Jensen, M. Bigler, R. Rothlisberger, H. Fischer, K. Goto-Azuma, M.E. Hansson, U. Ruth, J. Geophys. Res. 111 (2006).
[23] S. Sommer, D. Wagenbach, R. Mulvaney, H. Fischer, J. Geophys. Res. 105 (2000) 29423.
[24] B. Stenni, F. Serra, M. Frezzotti, V. Maggi, R. Traversi, S. Becagli, R. Udisti, J. Glaciol. 46 (2000) 541.
[25] S. Meinardi, I.J. Simpson, N.J. Blake, D.R. Blake, F.S. Rowland, Geophys. Res. Lett. 30 (2003) 1454.
[26] M. Bigler, S. Sommer, B. Stauffer, D. Wagenbach, H. Fischer, J. Kipfstuhl, H. Miller, Ann. Glaciol. 35 (2002) 250.
[27] H. Fischer, D. Wagenbach, J. Kipfstuhl, J. Geophys. Res. 103 (1998) 21935.
[28] P.A. Mayewski, W.B. Lyons, M.J. Spencer, M.S. Twickler, C.F. Buck, S. Whitlow, Nature 346 (1990) 554.
[29] D.E. Parker, Meteorol. Mag. 112 (1993) 184.
[30] M. Frezzotti, M. Pourchet, O. Flora, S. Gandolfi, M. Gay, S. Urbini, C. Vincent, S. Becagli, R. Gragnani, M. Proposito, M. Severi, R. Traversi, R. Udisti, M. Fily, Clim. Dynam. 23 (2004) 803.
[31] R.I. Cullather, D.H. Bromwich, M.L. Van Woert, J. Geophys. Res., 101 (D14) (1996) 19109.
[32] D.H. Bromwich, A.N. Rogers, P. Källberg, R.I. Cullather, J.W.C. White, K.J. Kreutz, J. Climate 13 (2002) 1406.
[33] E.A. Meyerson, P.A. Mayewski, K.J. Kreutz, L.D. Meeker, S.I. Whitlow, M.S. Twickler, Ann. Glaciol. 35 (2002) 430.
[34] A.M. Carleton, J. Geophys. Res. 108 (C4) (2003) 8080.
[35] N.A.N. Bertler, T.R. Naish, P.A. Mayewsky, P.J. Barrett, Adv. Geosci. 6 (2006) 83.
[36] N.A.N. Bertler, P.J. Barrett, P.A. Mayewski, R.L. Fogt, K.J. Kreutz, J. Shulmeister, Geophys. Res. Lett. 31 (2004) L15207.
[37] J. Turner, Int. J. Climatol. 24 (2004) 1.
[38] I. Simmonds, T.H. Jacka, J. Climate 8 (1995) 637.
[39] S.S. Jacobs, J.C. Comiso, J. Climate 10 (1997) 697.
[40] A.B. Watkins, I. Simmomds, J. Climate 13 (2000) 4441.
[41] R. Kwok, J.C. Comiso, Geophys. Res. Lett. 29 (2002).
[42] Welch, K.A., Glaciochemical investigations of the Newall Glacier, Southern Victoria Land, Antarctica. MSc. thesis, University of New Hampshire, 136 pp. (1993).
[43] M.A.J. Curran, T.D. van Ommen, V.I. Morgan, K.L. Phillips, A.S. Palmer, Science 302 (2003) 1203.
[44] A. Minikin, M. Legrand, J. Hall, D. Wagenbach, C. Kleefeld, E. Wolff, E.C. Pasteur, F. Ducroz, J. Geophys. Res. 103 (1998) 10975.
[45] J.A.E. Gibson, R.C. Garrick, H.R. Burton, A.R. McTargat, Mar. Biol. 104 (1990) 339.
[46] A. Vairavamurthy, M.O. Andreae, R.L. Iverson, Limnol. Oceanogr. 30 (1985) 59.
[47] G. Malin, S.M. Turner, P.S. Liss, J. Phycol. 28 (1992) 590.
[48] A. Gambaro, I. Moret, R. Piazza, C. Andreoli, E. Da Rin, G. Capodaglio, C. Barbante, P. Cescon, Int. J. Environ. Anal. Chem. 84 (2004) 401.

Please cite this article as: M. Severi, et al., Thirty years of snow deposition at Talos Dome (Northern Victoria Land, East Antarctica): Chemical profiles and climatic implications, Microchem. J. (2008), doi:10.1016/j.microc.2008.08.004